

Journal of Materials Chemistry B

Accepted Manuscript



This is an *Accepted Manuscript*, which has been through the Royal Society of Chemistry peer review process and has been accepted for publication.

Accepted Manuscripts are published online shortly after acceptance, before technical editing, formatting and proof reading. Using this free service, authors can make their results available to the community, in citable form, before we publish the edited article. We will replace this *Accepted Manuscript* with the edited and formatted *Advance Article* as soon as it is available.

You can find more information about *Accepted Manuscripts* in the [Information for Authors](#).

Please note that technical editing may introduce minor changes to the text and/or graphics, which may alter content. The journal's standard [Terms & Conditions](#) and the [Ethical guidelines](#) still apply. In no event shall the Royal Society of Chemistry be held responsible for any errors or omissions in this *Accepted Manuscript* or any consequences arising from the use of any information it contains.

ARTICLE

Preparation and characterizations of poly(2-methyl-2-oxazoline) based antifouling coating by thermally induced immobilization

Cite this: DOI: 10.1039/x0xx00000x

Longchao Bai, Lin Tan, Lijuan Chen, Songtao Liu, Yanmei Wang *

Received 00th January 2012,
Accepted 00th January 2012

DOI: 10.1039/x0xx00000x

www.rsc.org/

Poly(2-methyl-2-oxazoline) (PMOXA) has been proved to be a kind of potential antifouling coating material. In this work, a series of comb copolymers, poly[(2-methyl-2-oxazoline)-random-glycidyl methacrylate] (PMOXA-r-GMA) with a variety of compositions were synthesized by free radical polymerization of oligo(2-methyl-2-oxazoline)methacrylate macromonomer and glycidyl methacrylate, then characterized and used to coat silicon/glass surfaces. A one-step coating procedure by simple annealing protocol was used to yield covalent and cross-linked PMOXA-based antifouling coating. The coatings were rigorously characterized in terms of the surface chemical composition, hydrophilicity, thickness and morphology using X-ray photoelectron spectroscopy (XPS), water contact angle (WCA) test, ellipsometry and atomic force microscopy. The results demonstrated that the PMOXA-r-GMA brushes could successfully be bonded onto the silicon/glass surfaces. Finally, the fouling resistance ability of the modified surface was evaluated by analyzing the adsorption of bovine serum albumin protein, bacterial cell attachment and platelet adhesion, which indicated that the modified silicon/glass surfaces had superior resistance to protein, bacterial cell and platelet adsorption, and the performance of fouling resistance was enhanced with the content of PMOXA segments in the copolymers.

Introduction

The antifouling property is highly desirable for numerous biomedical and biomaterial applications including biosensors, biomedical devices, and drug delivery,¹⁻⁴ where the fouling is unfavorable for the performance of these surface-based devices. Such fouling can certainly limit the accuracy and precision of analysis and cause substantially increased energy consumption. Nonspecific protein adsorption is the focus of surface fouling due to the rapid adhesion of biomolecules such as protein adsorption is the first step of surface fouling. To date, significant amount of works dedicated to imparting high resistance to protein adsorption, are to build up a hydrophilic, highly hydrated, uncharged, polymer brush surface,^{5,6} ascribed to their outstanding water-trapping property, which will create a highly hydrated surface and lead to the inhibition of protein adsorption onto surfaces. Some of the most widely used protein-repelling materials are poly(ethylene glycol),^{7,8} zwitterionic,⁹⁻¹² and peptidomimetic polymers.^{13,14}

Recently, poly(2-methyl-2-oxazoline) (PMOXA), a peptidomimetic polymer has received growing attention for their promising characteristics as antifouling coating materials.¹⁵⁻²¹ The water-soluble PMOXA resembles the poly(ethylene glycol) (PEG) in structure and shows similar or better properties to PEG (e.g. hydrophilicity, biocompatibility),^{22,23} while it might be less prone to degradation than PEG.^{18,24,25} Additionally, PMOXA can be readily synthesized by living cationic ring-opening polymerization (CROP) with less labor

demanding. Moreover, this allows for designing and constructing polymers with multifunctional, well-defined architectures by incorporation of functional initiators, terminal groups, and particularly functional groups.^{21,26} On this account, PMOXA appears to be a promising candidate as antifouling coating material.

A significant challenge in designing antifouling surface is developing a method which enables the polymer to be robustly anchored. Covalent attachment of polymer offers better stability compared to physisorption methods. Two main methods for covalent attachment have emerged, namely “grafting to” and “grafting from”. The CROP used for PMOXA polymerization must be performed strictly within an inert atmosphere as it is sensitive to oxygen and water. Thus, the most common used method for anchoring PMOXA polymer brushes is “grafting to” method.^{15,16,20,27} On the other hand, the “graft to” method is convenient and simple to be implemented. We have prepared PMOXA brush coating using a multistep “graft to” method by immobilizing PMOXA onto various material surfaces (including silica, glass, and gold substrates) through polydopamine (PDA) anchored coating for the first time.¹⁵ However, this multi-step approach is relatively complicated, and a more efficient and simple approach is highly desired.

Glycidyl methacrylate (GMA) has attracted interest partly because of its reactive epoxide group, which can react with various functional groups (i.e., Si-OH, -NH₂, -COOH) on the surfaces of various substrates, such as wood, paper, textiles and silica, glass plates.²⁸⁻³⁰ At the same time, GMA can serve as a

cross-linkable monomer, which can be thermally cross-linked into a stable thin polymer film on surfaces, when consist in a coating.³⁰⁻³³ Moreover, epoxy-modified polymers can be easily synthesized by copolymerization with GMA.³⁴ Copolymers with GMA functional groups have been widely used as surface coating material, such as, Hailiang Zou et al. designed and prepared a novel functional diblock copolymer, poly(2, 2, 2-trifluoroethylmethacrylate)-block-poly-(glycidylmethacrylate)²⁸. Yan R. Hansen et al. developed a dually reactive block copolymer, poly(glycidylmethacrylate)-block-poly-(vinyl-dimethyl azlactone).³⁵ In these cases, the polymers could form stable coatings on silicon, cotton, or glass via annealing process. Hence, the usage of GMA to attach polymer brushes to surfaces is highly interesting.

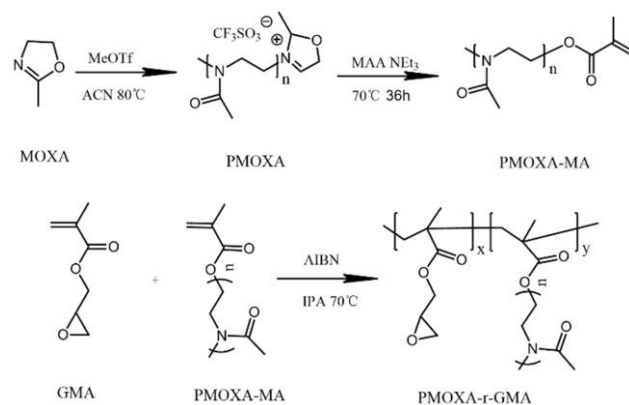
To meet the challenges for developing an antifouling surface by a simple, covalent approach, in this regard, a novel comb copolymer PMOXA-r-GMA with various compositions was designed and prepared. The synthesis of the comb polymers with an methacrylate backbone and PMOXA side chains involves the synthesis of a methacrylate end-capped oligo(2-methyl-2-oxazoline) methacrylate macromonomer (PMOXA-MA), followed by its copolymerization with GMA as the second step of the comb polymer synthesis (Scheme 1). In our comb polymer, the GMA segments can serve as an anchor by forming covalent bonds with the surfaces and self-crosslinking between GMA residues; whereas the long hydrophilic side chains composed of PMOXA segments can protrude into the aqueous medium and create a hydrated surface for preventing nonspecific adsorption of proteins. Ellipsometry, X-ray photoelectron spectroscopy (XPS), atomic force microscopy (AFM) and water contact angle measurement (WCA) were used to characterize the feature of copolymers functionalized surfaces, and evaluate the accomplishment of copolymers coated silicon/glass surface. Antifouling properties of the PMOXA-based surface were evaluated by protein adsorption, bacterial cell attachment and platelet adhesion.

Experimental

Materials

All water used in experiments was deionized water (LanLan Company, Hefei, China). 2-Methyl-2-oxazoline (MOXA, 99%, Sigma-Aldrich) was dried by refluxing over CaH₂ and subsequently distilled prior to use. Glycidyl methacrylate (GMA, 97%, Aladdin) was passed through an activated basic alumina column to remove the inhibitor before use. Methyl trifluoromethanesulfonate (MeOTf, 98%, Sigma-Aldrich) was distilled under reduced pressure and stored under nitrogen. Acetonitrile (ACN), methacrylic acid (MAA), trimethylamine (TEA), isopropanol (IPA) and other reagents were obtained from Sinopharm Chemical Reagents (China). TEA was dried over potassium hydroxide and distilled before use. MAA was distilled under reduced pressure. 2, 2'-Azobis (2-methylpropionitrile) (AIBN) was recrystallized from methanol. Labeled bovine-serum-albumin (BSA, Sigma-Aldrich) (FITC-BSA) was prepared by mixing BSA and fluorescein isothiocyanate (FITC, Sigma-Aldrich) at a molar ratio of 1:1 in Na₂CO₃-NaHCO₃ buffer for 2 h, followed by thorough dialysis in pH 7.4 phosphate-buffered saline (PBS, 10 mM) for three days. Escherichia coli ER2566 strain was kindly provided by Prof. Yangzhong Liu at the University of University of Science and Technology of China (Hefei, China). Silicon (111) wafers with a natural oxidized layer were received from Zhejiang Crystal Photoelectric Technology Co. (China).

Synthesis



Scheme1: synthesis of PMOXA-MA and PMOXA-r-GMA.

Oligo (2-methyl-2-oxazoline) methacrylate macromonomer

Oligo(2-methyl-2-oxazoline) methacrylate (PMOXA-MA) was synthesized in a manner analogous to that reported previously,³⁶ obtained in a similar fashion. Briefly, MeOTf (0.83 mg, 5 mmol), MOXA (5.03 g, 59.0 mmol) and 10 mL ACN were added into a 10 mL dried glass tube equipped with a magnetic stir bar. The mixture was degassed via three freeze-pump-thaw cycles. After the CROP was performed at 80 °C for 22 h, the end-capping agents MAA (0.64 mL, 7.2 mmol) and NEt₃ (1.4 mL, 10 mmol) were added, and the end-capping reaction was performed by heating the solution at 70 °C in an oil bath for 36 h. The mixture was then cooled to room temperature and the solvent was removed under reduced pressure. And then, the residue was dissolved in 20 mL of saturated NaHCO₃ aqueous solution and stirred for 30 min. Subsequently, the water in the mixture was extracted under reduced pressure, and 100 mL chloroform (CHCl₃) was added into the mixture and the mixture solution was stirred overnight. After that, the mixture solution was dried over sodium sulfate overnight, then filtrated, and concentrated under reduced pressure. The concentrated solution was added drop wise into the ice-cold diethyl ether to obtain the precipitation, and then the precipitation was dried in vacuo to give 4.3 g (76% yield) of white solid macromonomer (PMOXA-MA).

PMOXA-r-GMA

A series of PMOXA-r-GMA were synthesized via free radical polymerization with varied feed ratio of PMOXA-MA, GMA. As a typical example, PMOXA-MA (1 g, 1 mmol), GMA (35 μL, 0.25 mmol), and AIBN (4.1 mg, 0.025 mmol) were mixed in 10 mL of isopropanol in a 20 mL dried glass tube equipped with a magnetic stir bar. The mixture was degassed via three freeze-pump-thaw cycles and placed in an oil bath at 70 °C for 24 h with vigorous stirring. The polymerization was quenched by cooling the flask with cold water and exposure to air. Subsequently, the resulting viscous oil was diluted with 10 mL of chloroform, precipitated in cold diethyl ether, filtered off, and then dissolved in 10 mL of chloroform and precipitated again into diethyl ether. After that, the sample was dried in vacuum. Different mole ratios of PMOXA-MA (x) to GMA (y) (0.25–0.75) were used to synthesize three different copolymers denoted as PMOXA-r_{x/y}-GMA with three different monomer ratios (x/y) of 1/3, 1/1, and 3/1. The molar ratio of the

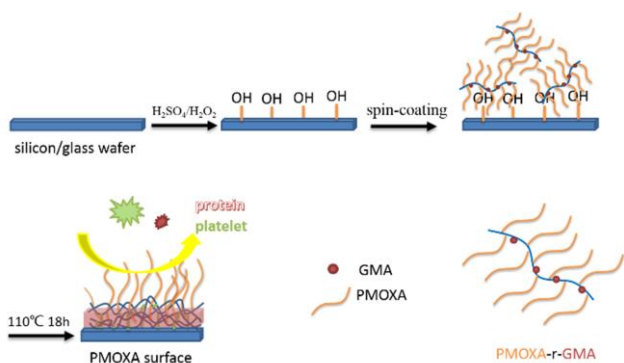


Fig. 1. Schematic illustration for the preparation of a PMOXA-r-GMA brush on the silicon/glass surface.

PMOXA-MA segment to GMA segment was determined by using ^1H NMR.

Surface modification

Silicon/glass wafers were cut into $1 \times 1 \text{ cm}^2$ pieces and cleaned by sonication in ethanol (15 min) and then in deionized water (15 min). Subsequently, the wafers were cleaned in piranha solution (7:3 v/v mixture of H_2SO_4 (95–98%) and H_2O_2 (30%)) for 60 minutes, rinsed extensively with water, ethanol, and then dried (*Caution: Piranha solution reacts violently with many organic materials and should be handled with great care!*). The procedure followed for the immobilization of PMOXA based copolymers on silicon/glass is showed in Fig 1. The procedure is similar to the strategy employed by Lokitz et al.,³⁰ thin polymer coatings were made by spin-coating (KW-4A, Institute of Microelectronics, Chinese Academy of Sciences) the PMOXA-r-GMA copolymers onto silicon/glass wafers (at 2500 rpm for 12 s) from dilute CHCl_3 solutions in concentrations 10 mg/mL. Subsequently, the coatings were immediately annealed for 18 h in a preheated oven at 110°C . After annealing, the modified wafers were allowed to cool to room temperature and sonicated in CHCl_3 using an ultrasonic cleaner for 20 minutes to remove the physical adsorbed polymers from the surfaces, and then dried with a stream of dry N_2 .

Characterizations

NMR spectroscopy

^1H NMR spectra of PMOXA-MA and PMOXA-r-GMA were recorded on a Bruker DMX-300 instrument at 300 MHz. Spectra were acquired at room temperature using a deuterated chloroform solvent and referenced to an internal tetramethylsilane (TMS) standard.

Water contact angle measurements (WCA)

The water contact angles were measured with a CA system (SL200KB, USA KINO Industry Co., Ltd, USA) at ambient temperature. Static contact angles (θ_s) were measured by $2 \mu\text{L}$ water droplets being delivered to the surface using a microliter syringe. Advancing (θ_{adv}) and receding angles (θ_{rec}) were measured with the sessile drop method by depositing a droplet of $1 \mu\text{L}$ on the surface, then increasing the volume to $10 \mu\text{L}$, finally decreasing it. Advancing angles were considered as the maximum angles observed during the droplet growth. Receding contact angles were measured in correspondence of the drop profile just before the contact surface reduction. Each sample

was measured at three random locations on the functionalized silicon surface to check its uniformity.

X-ray photoelectron spectroscopy (XPS)

The XPS data were collected on VG ESCALAB MK II X-Ray Photoelectron Spectrometer (VG Scientific Instruments, England) with Al ($K\alpha$) X-ray source (1486.6 eV). All spectra were calibrated by setting the signal of the aliphatic C signal at 284.7 eV (rather than 285.0 given the high proportion of aromatic carbon in the compounds).

Ellipsometry

Film thicknesses were measured using a variable angle spectroscopic ellipsometer (M-2000, Woollam Co., Inc., Lincoln, NE). The measurements were performed in the spectral range of 370–1000 nm at two different angles of incidence (65° and 75°). The analysis software CompleteEASE 4.81 was used to analyze all data. Thicknesses reported are the average of measurements made from at least three spots on the polymer-modified wafer. To fit the ellipsometric data, the optical constants (refractive index, extinction coefficient) of Si ($n=3.865$, $k=0.020$) and SiO_2 ($n=1.465$, $k=0$) were used to determine the SiO_2 layer thickness of the freshly cleaned silicon surfaces.³⁷ Each polymer layer was represented as a slab of uniform thickness having sharp interfaces and optical properties described by a Cauchy model (refractive index smoothly decaying with wavelength) assuming that the PMOXA-r-GMA layers had refractive indices of 1.45 at 632 nm.³⁸

Atomic force microscopy (AFM)

The surface topology and surface roughness values of unmodified, and polymer-modified silicon surface was performed on a DI Multimode V atomic force microscope (AFM) from Veeco Instruments (Mannheim, Germany). The microscope was operated in tapping mode using Si cantilevers with a resonance frequency of 273 kHz, a driving amplitude of 1.30V at a scan rate of 0.3 Hz. The AFM images were analyzed and post-processed using the NanoScope software (Version 5.12).

Antifouling

Evaluation of protein adsorption by fluorescence imaging

BSA conjugated with fluorescein isothiocyanate (FITC-BSA) was chosen as model protein for the evaluation of protein adsorption.³⁹ A total of 0.5 mg/mL protein solution was prepared by dissolving FITC-BSA in PBS (pH 7.4, 10 mM). Bare and coated glass wafers were incubated in FITC-BSA solution in a dark condition for 2 h at 37°C , and then washed with PBS and deionized water for three times, respectively, to remove the weakly bound proteins. Fluorescence images of FITC-BSA adsorbed samples were examined using optical microscope Olympus BX81 (Olympus, Japan) equipped with a halogen lamp, filter U-MNG2 ($\lambda_{\text{exit}} = 470\text{--}490 \text{ nm}$, $\lambda_{\text{emit}} > 510 \text{ nm}$) and camera type DP72. Color intensity was measured using image J software and an average value was calculated.⁴⁰ The relative adhesion amount of FITC-BSA was determined qualitatively based on the color intensity of fluorescence images.

Bacterial cell adhesion

Escherichia coli ER2566 strain was grown overnight in Luria-Bertani (LB) at 37°C on a rotary shaker (250rpm). Cells were

harvested by centrifugation at 4000 rpm for 10 min at 4 °C. The bacterial cells were washed with PBS (pH 7.4) and resuspended in PBS at a concentration of 10^8 cells mL^{-1} , as estimated from optical density (OD) at 600 nm (OD of 0.5 at 600nm is equivalent to $\sim 10^8$ cells mL^{-1}). The pristine and modified wafers were placed in a 6-well plate and covered with bacterial suspension (1 mL) at 37 °C for 4 h. All the samples were sterilized with UV irradiation for 1 h prior to the experiment. After the bacterial adhesion process, the wafers were washed thrice with PBS to remove the non-adherent bacteria. Gram-stain method was used to analyze bacterial adhesion. The crystal violet, iodine solution, decolorizer and safranin solution were used in Gram-stain. After bacterial stain, specimens were dried and the bacterial adhesion was observed by optical microscope Olympus BX81 (Olympus, Japan).

Platelet adhesion

The platelet adhesion measurement was carried out according to the standard protocol as described briefly below.^{41, 42} Fresh whole blood was collected from healthy volunteers in a 5.0 mL vacuum tube containing sodium citrate (109 mM) as the anti-coagulant (anti-coagulant to blood ratio, 1:9, v/v). The whole blood was then centrifuged at 1200 rpm for 15 min to obtain the platelet-rich plasma (PRP). The bare and modified surfaces were incubated with PRP for 2 h at 37 °C. After rinsing with PBS solution three times, the adhered platelets were fixed by 2.5% glutaraldehyde (v/v, in PBS) for 30 min. The samples were rinsed again with PBS solution and dehydrated by 25%, 50%, 75%, 90%, 100% ethanol solutions for 20 min each, in sequence. The samples were gold sputtered in a vacuum and then observed by scanning electron microscopy (SEM, JSM—6700F, JEOL, Japan) at a 5 KV accelerating voltage.

Stability study

To investigate their stability, the PMOXA-r-GMA-modified silicon/glass surfaces were preserved in a physiological buffer (PBS, pH=7.4, 10mM) solution at ambient environment for three weeks. The coating stability was monitored by three different surface characterization techniques, i.e. water contact angle (CA), X-ray photoelectron spectroscopy (XPS) and Fluorescence Imaging. CA allows for a determination of surface hydrophilicity. XPS provides chemical information of the studied surfaces. Fluorescence Imaging was used to monitor the non-fouling properties of the copolymer films before and after stability test. All the tests followed the procedures described above.

Results and discussion

Preparation and characterization of PMOXA-r-GMA

In this work, the initial step in the comb copolymers synthesis was the preparation of the oligo(2-methyl-2-oxazoline) methacrylate macromonomer (PMOXA-MA) with a degree of polymerization (DP) of 11 by direct end-functionalization of the cationic oxazolinium species present after the CROP of MOXA. The CROP was terminated by addition of a methacrylate nucleophile, which was formed in situ by deprotonation of MAA with TEA, as depicted in Scheme 1. The successful end functionalization is confirmed by ¹H NMR spectroscopy, clearly showing the presence of the two vinylic protons of the methacrylate end group at 5.62 and 6.10 ppm as well as the methylene protons next to the ester functionality at 4.29 ppm (Fig. 2 A). Comparison of the peak integrals derived

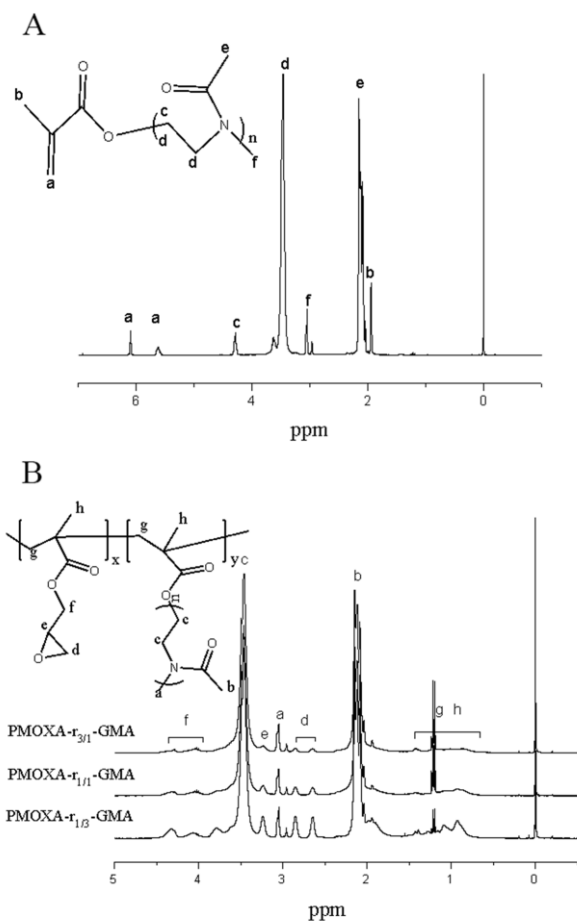


Fig. 2 ¹H-NMR spectrum of PMOXA-MA (A) and PMOXA-r-GMA with different composition (B).

from the vinylic protons with the α -terminal methyl group signal at 3.05 ppm reveals a degree of functionalization of 100% and additionally confirms the targeted DP of the macromonomer by integration of the PMOXA backbone signal around 3.46 ppm. PMOXA-r-GMA copolymers were synthesized via conventional radical polymerization method with AIBN as the initiator. The feed molar ratio of the PMOXA-MA in copolymers ranges from 25% to 75%. The route of synthesis is depicted in Scheme 1. Fig. 2 B is the ¹H NMR spectra of the PMOXA-r-GMA copolymers with different monomer feed ratio together with the assignment

Table 1. Copolymers composition

Polymer abbreviation ^a	Monomer feed ratio [PMOXA-MA]/[GMA]	Polymer composition ^b [PMOXA-MA]/[GMA]
PMOXA-r3/1-GMA	1:0.33	1: 0.51
PMOXA-r1/1-GMA	1:1	1:1.35
PMOXA-r1/3-GMA	1:3	1: 2.85

a: the numbers in subscript represent the monomer ratio of [PMOXA-MA]/[GMA].

b: the values determined by using ¹H NMR.

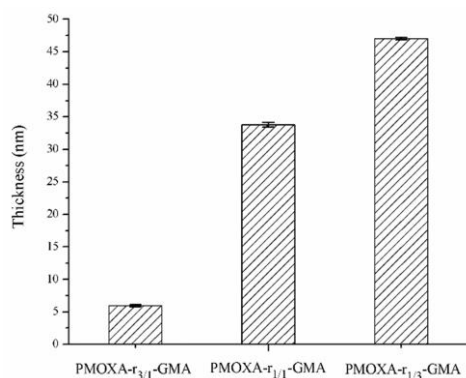


Fig. 3. Thickness of polymer coating. Data are expressed as mean \pm SD (n = 3), P < 0.01.

of the spectrum. The peaks of resonance at 2.63, 2.84 and 3.24 ppm were assigned to the protons of methylene and methine of GMA epoxide group, individually; and the signals of protons for the methylene connected to epoxide groups was detected at 3.98 and 4.30 ppm. In addition, the peak of resonance at 2.07 ppm was ascribed to methyl protons connected to amide group and the signal of resonance at 3.45 ppm was attributed to the protons of methylene in the main chain of PMOXA side chain. Thus, the ^1H NMR spectroscopy indicates that the resulting copolymer combined the structural features from GMA and PMOXA sections. Chemical composition of the copolymers was also verified by ^1H NMR. The peak at 2.63, 2.84 representative of GMA decreased from PMOXA-r_{1/3}-GMA to PMOXA-r_{3/1}-GMA with the feed molar ratio of the GMA decreasing. Relative areas of the two peaks corresponding the PMOXA side chains (a, $\delta \approx 3.05$) and GMA groups (d, $\delta \approx 2.63$ and $\delta \approx 2.84$) were used to determine the molar percentage of PMOXA-MA and GMA in each copolymer. The polymer compositions determined by ^1H NMR are presented in Table 1. The compositions of resulting copolymers were close to the feed molar ratio. From PMOXA-r_{3/1}-GMA to PMOXA-r_{1/3}-GMA, the GMA contents in the copolymers were continuously increased, while the PMOXA contents were continuously decreased.

Surface characterization of modified substrates

Table 2. The atomic percentage of elements on the bare and three copolymer modified surfaces based on XPS and corresponding static, advancing and receding water contact angle

	Element mole percent (atom %)				N/C	Contact angle ($^\circ$) ^a			
	O (1s)	N (1s)	Si (2s)			θ_s	θ_{adv}	θ_{rec}	$\Delta\theta$
bare silicon wafer	7.36	53.47	0	39.15	0	67.7 \pm 3.3	80.9 \pm 1.4	57.1 \pm 1.7	23.8 \pm 1.6
PMOXA-r _{3/1} -GMA -silicon wafer	56.14	23.66	10.76	9.44	0.192	23.4 \pm 1.3	31.3 \pm 1.8	10.2 \pm 1.4	21.1 \pm 1.6
PMOXA-r _{1/1} -GMA -silicon wafer	66.52	22.14	9.77	1.58	0.146	45.1 \pm 1.2	50.4 \pm 2.2	17.9 \pm 1.7	32.6 \pm 2.0
PMOXA-r _{1/3} -GMA -silicon wafer	68.34	23.65	7.48	0.53	0.109	59.2 \pm 1.9	80.1 \pm 2.6	27.9 \pm 3.1	52.2 \pm 2.9

a: Data are expressed as mean \pm SD (n = 3).

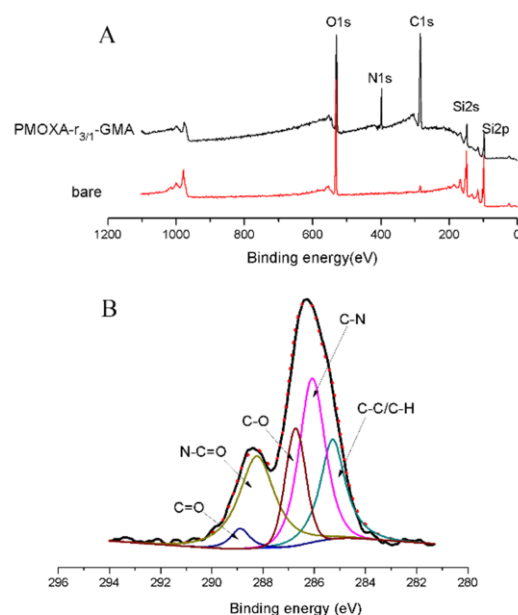


Fig. 4. XPS spectra of wide scan for the surfaces: bare and PMOXA-r_{3/1}-GMA-coated silicon wafer (A), and the high-resolution C1s of polymer brushes (PMOXA-r_{3/1}-GMA) (B).

The three random copolymers listed in Table 1 were coated on glass/silicon by spin-coating, followed by annealing and washing, as described in Experimental. The resulting coated surface was transparent and uniform in all cases. The coating thickness evaluated with an ellipsometer is shown in Fig. 3. As we can see, the thickness increased with the increment of GMA content. GMA can induce self-cross-linking among PMOXA-r-GMA chains when annealing the coating. Therefore, the copolymers with higher content of GMA segments allowed more chains farther from the silicon/polymer interface to be incorporated into the film, resulting in thicker coatings.

The surface chemical compositions of the silicon surface before and after the modification using PMOXA-r-GMA with different feed compositions were also studied with XPS. A comparison of the survey spectra for an unmodified silicon surface and PMOXA-r_{3/1}-GMA-modified surfaces illustrated changes in carbon (C1s, 287 eV), nitrogen (N1s, 400.5 eV), oxygen (O1s, 533 eV), and silicon (154 eV for Si2s and 103 eV

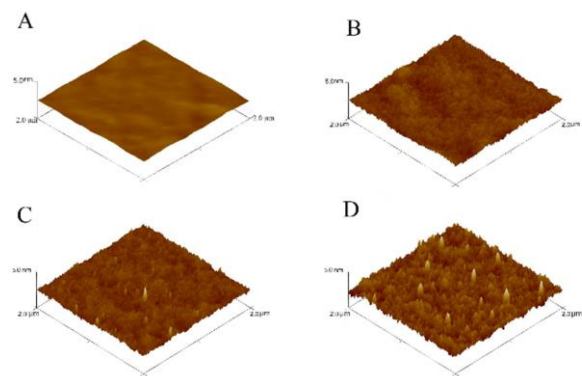


Fig. 5. AFM images of the silicon wafer before (A) and after (B-D) PMOXA- $r_{3/1}$ -GMA, PMOXA- $r_{1/1}$ -GMA, PMOXA- $r_{1/3}$ -GMA modification. The scan size was $2 \times 2 \mu\text{m}$, the vertical scale bars was 20 nm.

for Si2p) composition is shown in Fig 4 A. There were sharp increases in the N1s (400.5 eV) and the C1s (287 eV) peaks, and a decrease in the Si 2p peak for the PMOXA- $r_{3/1}$ -GMA modified surface compared to bare silicon surface, indicating the successful formation of PMOXA-based coating. Besides, Fig. 4 B shows the C 1s core-level spectra of PMOXA- $r_{3/1}$ -GMA modified wafer. The peak C1s can be resolved into five components for the carbon. The peaks of 285.0, 285.6, 286.2, 288.2 and 288.8 eV are mainly attributed to C-C/C-H, C-N, C-O, N-C=O and C=O groups, respectively.^{43, 44} The appearance of the peak assigned to C-N bonds at 285.6 eV, stemming from PMOXA side chains of the polymer brushes, indicates the introduction of the PMOXA- r -GMA polymer brush on the surfaces. We also did the same XPS analysis for bare silicon surface and the other two copolymers functionalized surfaces, and the results are summarized in Table 2. The surface of the bare silicon after “piranha” solution treatment was mainly composed of O and Si derived from surface oxides. These results were in good agreement with those reported in the literature.⁴⁵ From the data of the modified surface (PMOXA- $r_{3/1}$ -GMA, PMOXA- $r_{1/1}$ -GMA and PMOXA- $r_{1/3}$ -GMA), we could find that the nitrogen (N) concentration increased with the increment of PMOXA content in copolymers,

revealing that the density of the hydrophilic PMOXA brushes on the surface was increasing from PMOXA- $r_{1/3}$ -GMA to PMOXA- $r_{3/1}$ -GMA. The coverage degree of silicon (Si) signal improved with the increase in GMA content was consistent with the results of coating thickness, which also increased with the increment of the content of GMA. Furthermore, the N/C value increased from 0.120 to 0.192 with the increase of PMOXA contents from PMOXA- $r_{1/3}$ -GMA, PMOXA- $r_{1/1}$ -GMA to PMOXA- $r_{3/1}$ -GMA, indicating that the PMOXA contents increased on the surfaces. All these results indicated that the surface was covered with the PMOXA based copolymers and the PMOXA brushes on the PMOXA- $r_{3/1}$ -GMA-coated surface were the richest.

To further characterize the grafting of PMOXA-based polymers on the surface, the surface morphology was studied by tapping-mode AFM and the corresponding three-dimensional images are shown in Fig. 5. It was noticed that the surface morphology had been altered with coating of the three PMOXA- r -GMA copolymers with different compositions, compared with the bare silicon surface. In the case of the bare silicon surface, a smooth surface morphology was observed with root-mean-squares (RMS) roughness of 0.230 nm (Fig 5A). While the images Fig 5B-D indicate an increase in roughness with the RMS values increasing to 0.315nm, 0.384nm, 0.518 nm, respectively, after subsequent grafting of the three copolymers, revealing the presence of the copolymer layer on the surface.

Hydrophilicity of the copolymer coatings

Water contact angle measurement is the most convenient way to assess the hydrophilicity and wettability of solid surface, and the hydrophilicity is a commonly used parameter to determine the antifouling properties of the surface. From the results presented in Table 2, it was seen that the bare silicon wafer after annealing had a static contact angle of 67.7° and the values of the modified wafers have been found to consistently decreased to 59.2° , 45.1° and 23.4° for PMOXA- $r_{1/3}$ -GMA, PMOXA- $r_{1/1}$ -GMA and PMOXA- $r_{3/1}$ -GMA brushes, respectively. The apparent increase in hydrophilicity can be attributed to the introduction of hydrophilic PMOXA brushes on the surfaces, and the results are in good agreement with the conclusion of XPS, in which it was found the amount of the hydrophilic PMOXA brushes increased from PMOXA- $r_{1/3}$ -

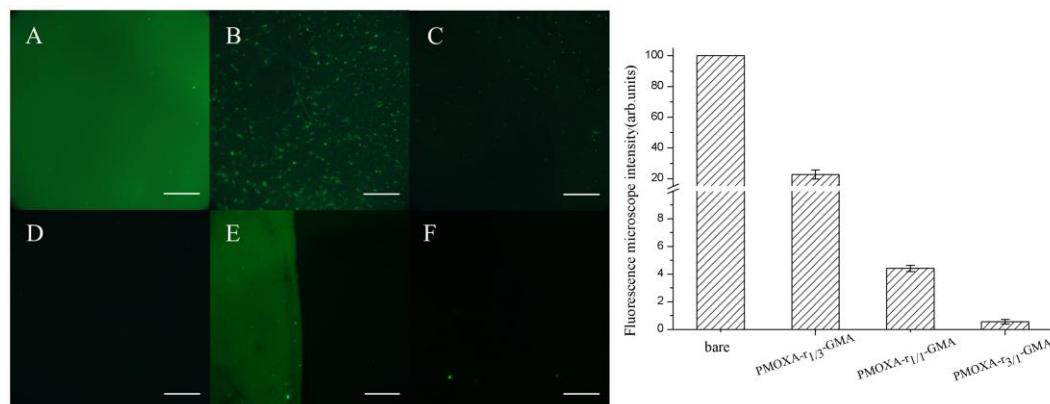


Fig. 6. Fluorescence microscopy intensity results of BSA-FITC incubated samples. (A) pristine glass wafer (Si/SiO₂), (B) PMOXA- $r_{1/3}$ -GMA, (C) PMOXA- $r_{1/1}$ -GMA modified wafer, (D) PMOXA- $r_{3/1}$ -GMA modified wafer, (E) half PMOXA- $r_{3/1}$ -GMA-modified wafer, (F) PMOXA- $r_{3/1}$ -GMA modified wafer after incubating in PBS three weeks. The bar graph gives the relative fluorescence intensity of the four samples when the pristine glass wafer (Si/SiO₂) controls normalized to 100. (magnification are 40, bars are 50 μm). Data are expressed as mean \pm SD (n = 3).

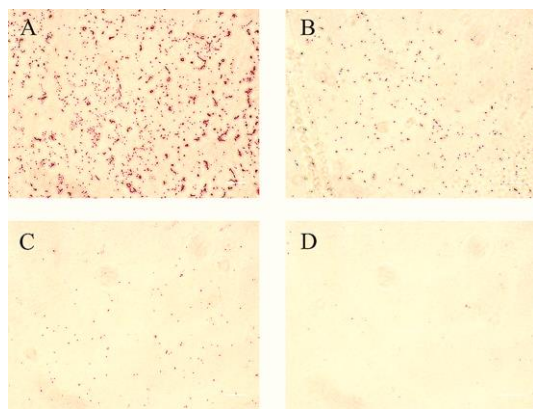


Fig. 7. Microscopic images of the stained bacteria attached to (A) pristine glass wafer (Si/SiO₂), (B) PMOXA-r_{1/3}-GMA-modified, (C) PMOXA-r_{3/1}-GMA-modified, and (D) PMOXA-r_{3/1}-GMA modified wafer (bars are 10 μm).

GMA, to PMOXA-r_{1/1}-GMA and PMOXA-r_{3/1}-GMA-modified surface. Meanwhile, measurements of the advancing and receding contact angles were conducted for the copolymer-modified surfaces (as shown in Table 2). The increase of high surface energy PMOXA segments caused a drop in the receding angle from 27.9° to 10.2°. The small hysteresis ($\Delta\theta$, 21.1°) indicates a smooth and chemically homogeneous surface of the PMOXA-r_{3/1}-GMA surface,⁴⁶ consistent with the above AFM results. Additionally, the result is particularly striking that PMOXA-r_{3/1}-GMA coating exhibited the best hydrophilic property. Herein, it can be speculated that PMOXA-r_{3/1}-GMA-modified wafer has promising fouling resistance ability because more hydrophilic surfaces is less prone towards fouling.⁴⁷

Antifouling properties of the modified surfaces

To qualitatively assess the protein adsorption, a fluorescence test was performed using FITC-BSA as a model protein according to the procedure described by Ciampi et al.⁴⁸ BSA was chosen due to its strong adsorption characteristics on various types of materials as previously described.⁴⁹ Fig 6(A-D) shows the surface images by fluorescence microscopy after 2 h of immersion in the fluorescein-labelled BSA protein solution (BSA-FITC). The bar graph is a relatively quantitative analysis of the fluorescence intensities in the corresponding images in Fig. 6. Intense fluorescence (appearing green) was observed in the non-modified glass surface, confirming that the BSA was efficiently adsorbed on the bare surface, whereas the modified samples showed substantially reduced fluorescence. It can be concluded that the presence of hydrophilic PMOXA chains on the surface was responsible for the reduction in protein adsorption. On the other hand, we can find from Fig 6(A-D) that the amount of the adsorbed BSA-FITC dramatically decreased with the increasing of the PMOXA content that was consistent with the hydrophilicity sequence of PMOXA-r-GMA coating obtained from water contact angle measurements. As expected, the lowest fluorescence intensities were observed on PMOXA-r_{3/1}-GMA modified surface (Fig 6D), indicating high resistance to BSA adsorption, corresponding to the hydrophilic nature of its surface. In order to reflect the antifouling performance more clearly, the half PMOXA-r_{3/1}-GMA-modified glass wafer (Fig 6E) was prepared, and we can find that the right half with PMOXA-r_{3/1}-GMA coating showed obvious improved protein resistance ability.

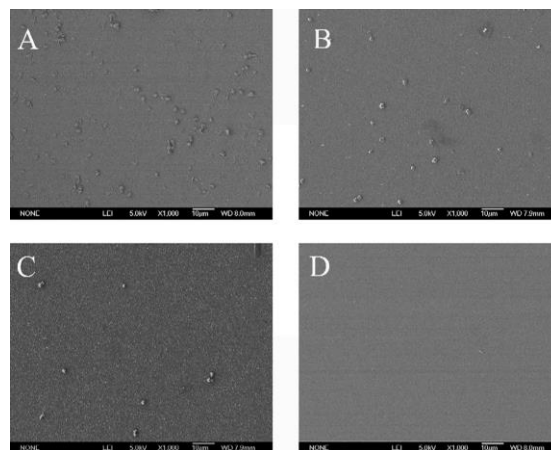


Fig. 8. SEM images of the adhesion of blood platelets on the surface of original (A) and PMOXA-r_{1/3}-GMA, PMOXA-r_{1/1}-GMA, PMOXA-r_{3/1}-GMA immobilized silicon wafers after incubating in fresh human PRP for 120 min (B, C, D) with the magnification of 1000.

Bacterial attachment is the first prerequisite for biofilm formation. Therefore, we tested the attachment of the gram negative bacterium *Escherichia coli* ER2566. Fig 7 shows representative microscopic images of the stained bacteria attached to the unmodified and modified glass surfaces. A strong decrease in bacteria density at the surface (Fig 7 B-D) was observed with the increasing of the PMOXA content, indicating a clear inhibitory effect on bacteria attachment of the PMOXA brushes. Our results show that the coating of PMOXA-r_{3/1}-GMA confers effective antifouling characteristics to the surface.

When materials contact with blood, proteins were first adsorbed instantaneously onto surfaces and deformed; then platelets were adsorbed, activated, and aggregated.⁵⁰ Thus, platelet adhesion on a substrate is another important tool for evaluating the protein repellent ability. Besides, a study on platelets adsorption was important to evaluate the blood compatibility of materials. Fig. 8 shows SEM images of platelets that adhered to the surfaces by contact of the prepared substrates with PRP solution for 120 min at 37 °C. A diminishing trend could still be found in platelet adhesion. Fig. 8A shows that there was significant adhesion of platelets on the bare silicon surface. In contrast, the PMOXA-r_{3/1}-GMA, 75 mol % PMOXA modified surface (Fig. 8D) had excellent resistance to platelet adhesion. The resistance of platelet adhesion was ascribed to the improved hydrophilicity and antifouling property after PMOXA-r_{3/1}-GMA immobilization. Thus, the platelet adhesion test revealed that surfaces modified by the PMOXA based copolymer could improve protein resistance property and biocompatibility upon direct exposure to plasma environment when compared with the original silicon wafer, and the coating could be useful in blood contacting surface.

In addition, it should be mentioned that during the reported coating method the unreacted GMA segments are able to bind proteins.⁵¹⁻⁵³ While the fact that PMOXA-r_{3/1}-GMA modified surface inhibited protein and platelets adhesion suggests that PMOXA chains have completely covered the surface and shielded the effect of unreacted GMA residues.

Stability of PMOXA based coating

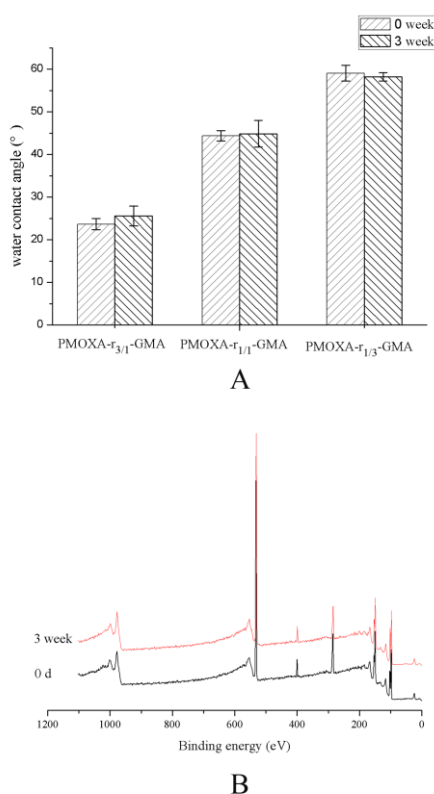


Fig. 9. The static contact angle for PMOXA-r-GMA-modified surfaces, $p < 0.05$ (A) and XPS analysis for PMOXA-r_{3/1}-GMA-immobilized surface performed before and after immersing the coated surface 3 weeks in PBS at room temperature (B).

The stability and durability of the PMOXA-based coating are examined by incubating the modified surfaces in PBS (pH=7.4, 10 mM) at the room temperature for 3 weeks in this work. The PBS was replaced weekly. Firstly, we investigated the changes of static water contact angle of each sample, which is presented in Fig. 9A. A slight change in static water contact angle is observed for the three samples after continuously incubating in PBS for 3 weeks. For example, the static water contact angle increased from 23.6° to 25.6° for PMOXA-r_{3/1}-GMA modified surface; from 44.3° to 44.9° for PMOXA-r_{1/1}-GMA modified surface and decreased from 59.1° to 58.2° for PMOXA-r_{1/3}-GMA modified surface suggesting good stability for all samples, due to the covalent anchoring and cross-linking of the GMA residues. In addition, we did further study for the stability of the PMOXA-r_{3/1}-GMA modified surface (with best protein-repellent properties). Seen from Fig. 9B as well as Fig. S1 (in the ESI, Electronic Supplementary Information), there is no obvious change in XPS wide spectra and the high-resolution C1s spectra of PMOXA-r_{3/1}-GMA-coated surface before and after incubating. This means few polymers can be removed from the coating during stability test. Furthermore, protein repellent properties (Fig. 6F) of PMOXA-r_{3/1}-GMA-coated surface also did not change much, with only a minor fluorescent signal observed after incubating in PBS for 3 weeks. In order to further illustrate the antifouling ability of PMOXA-r-GMA, poly(ethylene glycol) methyl ether methacrylate-random-glycidyl methacrylate (PEGMA-r_{3/1}-GMA) as a control polymer was prepared (as described in the ESI, Fig S2.) and used to coat on glass/silicon surface with the same method. We found that an obvious increase in fluorescent signal of BSA-

FITC was observed on PEGMA-r_{3/1}-GMA modified surfaces after incubating in PBS only one week, as presented in the ESI Fig S3B, for PEG is prone to degradation compare to PMOXA as previous reported^{18, 24, 25}. In effect, some fluorescent signal was observed (ESI, Fig S3A.) on the fresh PEGMA-r_{3/1}-GMA modified surfaces after BSA-FITC adsorption, for the typically elevated temperature during the annealing process probably lead to the oxidative degradation of PEG. All results implied that the PMOXA-r-GMA coatings possess a good stability for long-term and a better long-term anti-fouling property in physiological environment, which was attributed to the covalent anchoring and cross-linked structure.

Conclusion

In this paper, a series of comb-like copolymers of PMOXA-r-GMA with different PMOXA/GMA molar ratios were prepared by combination of living cationic ring-opening polymerization (CROP) and free-radical polymerization method. PMOXA we proposed here have many advantages such as good hydrophilicity, biocompatibility and high stability. An alternative approach was developed to covalently immobilize the PMOXA-r-GMA copolymers on silicon/glass wafers. The immobilization is carried out by a simple spin-coating and annealing procedure, and the results of XPS, AFM and water contact angle measurement confirmed that the PMOXA-r-GMA copolymer was successfully immobilized onto silicon/glass surface, and the improved hydrophilicity of the PMOXA-r-GMA copolymer modified silicon/glass surface was also demonstrated. The antifouling tests showed that the bio-fouling adsorption decreased with the increasing content of PMOXA in the copolymers. The PMOXA-r_{3/1}-GMA, with 75 mol % PMOXA surface demonstrated efficient resistance to single protein adsorption (BSA) as well as bacteria cell and platelets adsorption from human blood. In addition, the copolymer coating exhibited long-term stability against PBS. The process can be readily applied to the fabrication of where the covalently immobilized polymer brushes serve as the fouling-resistance surface.

Acknowledgements

This work was supported by the National Natural Science Foundation of China under Grant No. 21374109, and Ministry of Science and Technology of China under Grant No. 2012CB933802.

Notes and references

CAS Key Laboratory of Soft Matter Chemistry, Department of Polymer Science and Engineering, University of Science and Technology of China, Hefei 230026, P. R. China

*Corresponding author: Professor Yanmei Wang, Department of Polymer Science and Engineering, University of Science and Technology of China, Hefei 230026, P. R. China. Tel.: +86-551-63607652; Fax: +86-551-63601592; E-mail: wangyanm@ustc.edu.cn

1. C. Nogues, H. Leh, J. Lautru, O. Delelis and M. Buckle, *PLoS One*, 2012, **7**, e44287.
2. J. T. Santini, M. J. Cima and R. Langer, *Nature*, 1999, **397**, 335-338.
3. L. Mi, M. M. Giarmarco, Q. Shao and S. Jiang, *Biomaterials*, 2012, **33**, 2001-2006.
4. M. K. Leung, C. E. Hagemeyer, A. P. Johnston, C. Gonzales, M. M. Kamphuis, K. Ardipradja, G. K. Such, K. Peter and F. Caruso, *Angew. Chem. Int. Ed.*, 2012, **51**, 7132-7136.

5. I. Banerjee, R. C. Pangule and R. S. Kane, *Adv. Mater.*, 2011, **23**, 690-718.
6. M. Kobayashi, Y. Terayama, H. Yamaguchi, M. Terada, D. Murakami, K. Ishihara and A. Takahara, *Langmuir*, 2012, **28**, 7212-7222.
7. F. Khalil, E. Franzmann, J. Ramcke, O. Dakischew, K. S. Lips, A. Reinhardt, P. Heisig and W. Maison, *Colloids Surf B Biointerfaces*, 2014, **117**, 185-192.
8. R. Zeng, Z. Luo, D. Zhou, F. Cao and Y. Wang, *Electrophoresis*, 2010, **31**, 3334-3341.
9. L. Chen, L. Tan, S. Liu, L. Bai and Y. Wang, *J Biomater Sci Polym Ed*, 2014, **25**, 766-785.
10. T. Xiang, R. Wang, W. F. Zhao, S. D. Sun and C. S. Zhao, *Langmuir*, 2014, **30**, 5115-5125.
11. H. S. Sundaram, X. Han, A. K. Nowinski, J. R. Ella-Menye, C. Wimbish, P. Marek, K. Senecal and S. Jiang, *ACS Appl Mater Interfaces*, 2014, **6**, 6664-6671.
12. H. Yin, T. Akasaki, T. Lin Sun, T. Nakajima, T. Kurokawa, T. Nonoyama, T. Taira, Y. Saruwatari and J. Ping Gong, *J. Mater. Chem. B*, 2013, **1**, 3685-3693.
13. A. R. Statz, R. J. Meagher, A. E. Barron and P. B. Messersmith, *J. Am. Chem. Soc.*, 2005, **127**, 7972-7973.
14. S. Lin, B. Zhang, M. J. Skoumal, B. Ramunno, X. Li, C. Wesdemiotis, L. Liu and L. Jia, *Biomacromolecules*, 2011, **12**, 2573-2582.
15. L. N. Xiang, L. J. Chen, L. Tan, C. Zhang, F. H. Cao, S. T. Liu and Y. M. Wang, *Chin. Chem. Lett.*, 2013, **24**, 597-600.
16. R. Konradi, B. Pidhatika, A. Muhlebach and M. Textor, *Langmuir*, 2008, **24**, 613-616.
17. R. Konradi, C. Acikgoz and M. Textor, *Macromol. Rapid Commun.*, 2012, **33**, 1663-1676.
18. B. Pidhatika, J. Moller, E. M. Benetti, R. Konradi, E. Rakhmatullina, A. Muhlebach, R. Zimmermann, C. Werner, V. Vogel and M. Textor, *Biomaterials*, 2010, **31**, 9462-9472.
19. T. von Erlach, S. Zwicker, B. Pidhatika, R. Konradi, M. Textor, H. Hall and T. Lühmann, *Biomaterials*, 2011, **32**, 5291-5303.
20. K. Langowska, J. Kowal, C. G. Palivan and W. Meier, *J. Mater. Chem. B*, 2014, **2**, 4684-4693.
21. L. Tauhardt, K. Kempe, M. Gottschaldt and U. S. Schubert, *Chem. Soc. Rev.*, 2013, **42**, 7998-8011.
22. N. Adams and U. S. Schubert, *Adv Drug Deliver Rev*, 2007, **59**, 1504-1520.
23. R. Hoogenboom, *Angew. Chem. Int. Ed.*, 2009, **48**, 7978-7994.
24. B. Pidhatika, M. Rodenstein, Y. Chen, E. Rakhmatullina, A. Muhlebach, C. Acikgoz, M. Textor and R. Konradi, *Biointerphases*, 2012, **7**, 1.
25. Y. Chen, B. Pidhatika, T. von Erlach, R. Konradi, M. Textor, H. Hall and T. Lühmann, *Biointerphases*, 2014, **9**, 031003.
26. B. Guillermin, S. Monge, V. Lapinte and J. J. Robin, *Macromol. Rapid Commun.*, 2012, **33**, 1600-1612.
27. M. Agrawal, J. C. Rueda, P. Uhlmann, M. Muller, F. Simon and M. Stamm, *Acs Appl Mater Inter*, 2012, **4**, 1357-1364.
28. H. Zou, S. Lin, Y. Tu, G. Liu, J. Hu, F. Li, L. Miao, G. Zhang, H. Luo, F. Liu, C. Hou and M. Hu, *J. Mater. Chem. A*, 2013, **1**, 11246-11260.
29. E. Soto-Cantu, B. S. Lokitz, J. P. Hinestroza, C. Deodhar, J. M. Messman, J. F. Ankner and S. M. Kilbey, 2nd, *Langmuir*, 2011, **27**, 5986-5996.
30. B. S. Lokitz, J. Wei, J. P. Hinestroza, I. Ivanov, J. F. Browning, J. F. Ankner, S. M. Kilbey and J. M. Messman, *Macromolecules*, 2012, **45**, 6438-6449.
31. S. K. Schmitt, W. L. Murphy and P. Gopalan, *J. Mater. Chem. B*, 2013, **1**, 1349-1360.
32. D. P. Sweat, M. Kim, X. Yu and P. Gopalan, *Langmuir*, 2013, **29**, 3805-3812.
33. D. P. Sweat, M. Kim, X. Yu, S. K. Schmitt, E. Han, J. W. Choi and P. Gopalan, *Langmuir*, 2013, **29**, 12858-12865.
34. D. Wu, B. Zhao, Z. Dai, J. Qin and B. Lin, *Lab Chip*, 2006, **6**, 942-947.
35. R. R. Hansen, J. P. Hinestroza, K. R. Shubert, J. L. Morrell-Falvey, D. A. Pelletier, J. M. Messman, S. M. Kilbey, 2nd, B. S. Lokitz and S. T. Retterer, *Biomacromolecules*, 2013, **14**, 3742-3748.
36. S. Kobayashi, E. Masuda, S. Shoda and Y. Shimano, *Macromolecules*, 1989, **22**, 2878-2884.
37. S. Kinge, T. Gang, W. J. Naber, W. G. van der Wiel and D. N. Reinhoudt, *Langmuir*, 2010, **27**, 570-574.
38. O. Borozenko, C. Ou, W. G. Skene and S. Giasson, *Polym Chem*, 2014, **5**, 2242-2252.
39. A. J. Downard, S. L. Jackson and E. S. Tan, *Aust. J. Chem.*, 2005, **58**, 275-279.
40. M. Parviz, N. Darwish, M. T. Alam, S. G. Parker, S. Ciampi and J. J. Gooding, *Electroanalysis*, 2014, **26**, 1471-1480.
41. L. J. Zhu, L. P. Zhu, J. H. Jiang, Z. Yi, Y. F. Zhao, B. K. Zhu and Y. Y. Xu, *J Membr Sci*, 2014, **451**, 157-168.
42. Z. R. Xin, S. J. Yan, J. T. Ding, Z. F. Yang, B. B. Du and S. S. Du, *Appl. Surf. Sci.*, 2014, **300**, 8-15.
43. Y. T. Wei, Y. M. Zheng and J. P. Chen, *Langmuir*, 2011, **27**, 6018-6025.
44. W. J. Yang, K. G. Neoh, E. T. Kang, S. L. M. Teo and D. Rittschof, *Polym Chem*, 2013, **4**, 3105-3115.
45. S. J. Todd, D. J. Scurr, J. E. Gough, M. R. Alexander and R. V. Ulijn, *Langmuir*, 2009, **25**, 7533-7539.
46. À. Serrano, O. Sterner, S. Mieszkin, S. Zürcher, S. Tosatti, M. E. Callow, J. A. Callow and N. D. Spencer, *Adv. Funct. Mater.*, 2013, **46**, 5706-5718.
47. S. Chen, L. Li, C. Zhao and J. Zheng, *Polymer*, 2010, **51**, 5283-5293.
48. S. Ciampi, T. Bocking, K. A. Kilian, M. James, J. B. Harper and J. J. Gooding, *Langmuir*, 2007, **23**, 9320-9329.
49. W. J. Yang, T. Cai, K. G. Neoh, E. T. Kang, G. H. Dickinson, S. L. Teo and D. Rittschof, *Langmuir*, 2011, **27**, 7065-7076.
50. M. Gong, Y. B. Wang, M. Li, B. H. Hu and Y. K. Gong, *Colloids Surf B Biointerfaces*, 2011, **85**, 48-55.
51. W. Hu, Y. Liu, Z. Lu and C. M. Li, *Adv. Funct. Mater.*, 2010, **20**, 3497-3503.
52. C. Li, J. Jin, J. Liu, X. Xu and J. Yin, *RSC Adv*, 2014, **2014**, 24842-24851.
53. F. He, B. Luo, S. Yuan, B. Liang, C. Choong and S. O. Pehkonen, *RSC Adv*, 2014, **4**, 105-117.